ONLINE SUPPLEMENT

INCREASED PROTEOLYSIS, MYOSIN DEPLETION AND ATROPHIC AKT-FOXO SIGNALING IN HUMAN DIAPHRAGM DISUSE

Sanford Levine, M.D., Chhanda Biswas, Ph.D., Jamil Dierov M.D., Ph.D., Sc.D, Robert Barsotti, Ph.D , Joseph B. Shrager, M.D., Taitan Nguyen, B.S.E., Seema Sonnad, Ph.D., John C. Kucharchzuk, M.D., Larry R. Kaiser, M.D., Sunil Singhal, M.D., and Murat T. Budak, M.D., Ph.D.

TABLE OF CONTENTS

A. METHODS

SUBJECTS

Our protocol for case subjects was approved by the Gift of Life Donor Program (http://www.donors1.org), and our protocol for control subjects was approved by the University of Pennsylvania Institutional Review Board. All biopsy specimens were obtained with appropriate written informed consent.

DIAPHRAGM AND PECTORALIS MAJOR BIOPSIES

Full-thickness biopsy specimens were obtained from the same region of the right anterior costal diaphragm in all case and control subjects (1). The approximate sizes of diaphragm biopsies obtained from cases were 20 mm in length and 6-8 mm in width, whereas those from controls were 10 mm in length and 5 mm in width. In contrast, pectoralis major muscle full-thickness biopsies were 30 mm in length and 15 mm in width. Following removal, all diaphragm biopsies were kept at room temperature for 3-5 minutes to achieve length equilibrium, then frozen in isopentane, and then transferred to liquid nitrogen and stored at –80°C until used. Specimens from case subjects were obtained before circulatory arrest or removal of any organs, and specimens from control subjects were obtained during the surgery for their lung lesions.

In addition, to determine whether our hypothesis regarding atrophy was limited to the diaphragm, we obtained biopsy-specimens of the pectoralis major muscle at the level of the

third interspace in six cases and six control subjects. (These subjects were the only ones for whom appropriate consent was obtained for these biopsies.). To avoid surgical trauma to this superficial muscle, these pectoralis major specimens were obtained immediately after the skin incision, and processed in the same manner as the diaphragm specimens.

NUMBER OF SUBJECTS USED FOR DIFFERENT DIAPHRAGM MEASUREMENTS.

Figure E1 shows the number of subjects used for each of the measurements. The Figure shows that the twelve measurements in our protocol were carried out in six sequential steps (indicated by the rectangles in the Figure). The Figure indicates that a declining number of subjects were used in each sequential rectangle. The reason for this is that we progressively used up our specimens and therefore, only a small number of specimens were available for the latter measurements.

REAGENTS

The sources of common reagents used follows and their respective catalogue numbers are indicated in parentheses. The Complete protease inhibitor cocktail (11 836 170 001) and Phosphatase inhibitor cocktail set III containing Sodium Fluoride, Sodium Orthovanadate, Sodium Pyrophosphate, decahydrate and β-glycerophosphate (524627) were obtained from Roche Applied Sciences, Indianapolis, IN and Calbiochem Gibbstown, NJ, respectively. The Bicinchonic acid (BCA) assay reagent (23225) and micro-titer plates (237105) for protein estimation were purchased from Thermo Scientific, Rockfield, IL. The 4-12% Bis-Tris gradient gels (NP0321BOX) and sample buffer (NP007) for SDS-PAGE, protein A Agarose (15918-014) for

immunoprecipitation (IP) the 10% TBE (Tris-Borate-EDTA) native gel (EC62755BOX) for EMSA, Trizol reagent (15596-026) and Oligo(dt) primers (18418012) for qRT-PCR, were obtained from Invitrogen, Carlsbad, CA. The Hy-Bond-C nitrocellulose membrane (RPN303E) for immunoblot was purchased from GE Health care, Piscataway, NJ. The LightShift Chemiluminescent EMSA kit (20148) and Supersignal West Pico chemiluminescant substrate (34080) for Immunoblot were purchased from Pierce, Rockford, IL. The TransAM FKHR (FOXO1A) kit (46396) was obtained from Active motif, Carlsbad, CA. The 26S proteasome isolation kit, (Human 539176) was obtained from EMD Chemical, Inc. (Calbiochem, Gibbstown, NJ). The 20S proteasome activity assay kit (AK-740), and proteasome inhibitor—MG132 (PI-102)—were purchased from BIOMOL internationals, Plymouth Meeting, PA. For qRT-PCR analysis 2X Taqman gene expression master-mix (437006), FBX032-Atrogin1 (Hs0036970), TRIM63-MuRF-1 (Hs0082239) and Beta Actin (ACTB) (Hs9999990) were obtained from Applied Biosystems, Foster city, CA.

SOURCES OF ANTIBODIES

Antibodies against Ubiquitin (ab7780), α-Sarcomeric Actin (ab28052) were purchased from ABcam, Cambridge, MA; AKT (9272) and p-Serine 473 AKT (4058) were obtained from Cell Signaling Technology, Inc, Danvers, MA; FOXO1 (sc11350), and p-Serine 256 FOXO1 (sc22158-R) were obtained from Santa Cruz Biotechnology, Inc, Santa Cruz, CA; myosin heavy chain (fast) (M4276) from Sigma Aldrich, Saint Louis, MO; MyHC slow (NOQ7.54D, a generous gift from Dr. Neil Rubinstein, Univ. of Pennsylvania) and superoxide-dismutase-1 (SOD1) (SPC-116C) from StressMarq, Victoria, Canada. The horse radish peroxidase conjugated (HRP conjugated)

secondary antibodies used were either Rabbit IgG (NA934V) or Mouse IgG (NA931V) from GE Health care, Piscataway, NJ.

PREPARATION OF CYTOPLASMIC AND NUCLEAR PROTEIN FRACTIONS

Frozen diaphragm tissues (20-50 mg) were cut into small pieces with a clean razor blade, trimmed of connective tissues and fat, briefly minced in Tris buffered saline (TBS) containing the Complete Protease Inhibitor cocktail and the phosphatase inhibitor cocktail set III. The pellet obtained after cold-centrifugation (i.e. 4^{o}C) at 1000 rpm for 5 minutes was partitioned for cytosolic and nuclear proteins. The pellets were re-suspended in 400 µl of ice-cold lysis buffer (50 mM HEPES, pH 7.9, 10 mM NaCl, 10 mM KCl 1.0 mM Ethylene-diamine-tetraacetic acid (EDTA), 1.0 mM ethylene glycol-bis (beta-aminoethyl ether)-N,N,N',N'-tetraacetic acid (EGTA), 20 % glycerol, 1.0 mM Dithiothretol (DTT), 0.05% non-ionic detergent (NP-40)) containing the Complete Protease Inhibitor and phosphatase inhibitor set III. The samples were incubated for 15 min on ice with occasional mixing on vortex to promote release of cytoplasmic proteins in the soluble fraction. The samples were then cold centrifuged for 5 min at 6000 rpm. The supernatants of this centrifugation constituted our cytoplasmic fractions that were then stored at -80^{o}C until used. The pellets—resulting from the above centrifugations containing intact nuclei—were washed 3 times in ice-cold TBS, and then incubated on ice for 30 min with frequent mixing on vortex in 200µl of the same buffer used for cytoplasm extraction

supplemented with 28µl of 5 M NaCl. The lysates were then cold-centrifuged at 15,000 rpm for 15 min. These supernatants contained the nuclear proteins and were stored at -80^{o}C until used.

TEST FOR PURITY OF CYTOPLASM AND NUCLEAR PROTEIN FRACTIONS

To test the efficiency of separation of our nuclear and cytoplasmic protein isolations, we used myosin-1β as our nuclear marker protein and superoxide dismutase 1 (SOD1) as our cytoplasmic marker protein. All nuclear fractions contained no SOD1 and all cytoplasmic fractions contained no myosin-1β. Figure E2 in this supplement contains representative examples.

IMMUNOBLOT

Approximately 15-30 µg of protein from cytoplasmic and nuclear fractions of each diaphragm biopsy were resolved on 4-12 % Bis-Tris SDS-PAGE and transferred to nitrocellulose membranes. The membranes were Ponceau-stained to assess uniform transfer to the membranes. Subsequently, after removal of the Ponceau stain by water wash, purities of the nuclear and cytoplasmic fractions were ensured by probing with myosin-1β (a nuclear protein) and SOD-1 (a cytoplasmic protein) antibodies—see above paragraph.

Loading of lanes on gel. First, we measured the protein content of nuclear and cytoplasmic fractions by carrying out bicinchoninic acid assay (BCA) and then we calculated the amount of lysis buffer to effect approximately equal protein concentration and roughly equal

volumes in each lane of gel. Each gel was loaded with an equal number of case and control samples in a sequential manner with 6 control specimens followed by 6 cases until specimens were all loaded.

Transfer of proteins to membranes. Unless otherwise indicated in the text, each single gel was then placed in an electroblotter, (Idea Scientific, Corvalis OR) and protein was transferred to nitrocellulose membranes using a constant voltage of 12V for 15 hours at 4^{o}C. In some instances-as noted in text—two gels to be analyzed for the same protein molecules were placed in the same cassette and underwent transfer under the same conditions for the identical period of time. We assured completeness of protein transfer to the nitrocellulose membrane by staining the gel following electrophoretic transfer with Coomassie stain for any residual protein; none was found in any of our transfers in these studies.

Protein transfer to each lane of same membrane. To ensure approximately equal transfer of protein to each lane, we stained each membrane with Ponceau staining. Based on the densitometric analysis of the Ponceau stain, the lane to lane variation on the same gel—including that between cases and controls on the same gel—was less than 10%. Additionally, samples from different gels that were transferred to the membrane were also less than 10%. These data suggest that protein transferred from two different gels—under these identical conditions—do not produce any additional variation in protein transferred to gel.

After removal of the Ponceau stain by water wash, we probed the nitrocellulose membranes with appropriate primary antibodies to proteins of interest as well as our loading controls. We then added appropriate HRP–conjugated secondary antibodies and exposed each

membrane to x-ray films sequentially for at least four different time points to assure the linearity of the OD versus the time of exposure relationship. Importantly, we noted that the loading control did not differ between lanes by more than 10%.

Quantification of immunoblot data. The membranes within Figures 4-7 in the text and Figures E2 and E3 and data in Figure E4 in Online Supplement were obtained by exposure to X-ray films at 4 different time intervals to ensure that our measurements were made in the linear range of the time of exposure versus OD. The data shown in Figures 1 and 3 were measured by Odyssey (Li-COR Biosciences) using fluorescence tagged secondary antibodies (Odyssey Goat anti Rabbit IRDye 680 and Odyssey Goat anti-mouse IRDye 800). The membranes were exposed at different intensities equivalent to different time exposure to obtain data within linear range. We quantified our protein bands of interest using the Image Processing and Analysis in Java (Image J) software provided online (http://rsbweb.nih.gov/ij/) by NIH. Unless otherwise indicated, all measurements of the same protein were carried out at the same exposure time.

Special Considerations regarding gels and protein transfer. Depending on the number of samples used for each measurement, we either made our own gels or we bought precast gels (15wells) from invitrogen (NP0321BOX). If the number of samples exceeded 12, we casted our own gels using a gel casting system (16x14 cm) (FB-GC16-1, Fisher Scientific, Pittsburgh PA). We were able to make gels having various numbers of wells by using different combs up to a maximum of 25 wells. When adequate specimens were available, we used 6 case and 6 control samples for a portion of our initial run. In those cases where additional samples were available,

we ran these additional samples on a second gel (having an appropriate number of wells). We realize that this is a somewhat unconventional procedure; however, we present data in RESULTS that demonstrate that this two gel methodology does not introduce artifact.

MEASUREMENT OF DNA-FOXO BINDING

We first used electrophoretic mobility shift assay (EMSA) to check the binding of FOXO 1 and then for a more quantitative assay we used a modified enzyme-linked immunosorbent assay (ELISA) using the TransAM FKHR (FOXO1) kit (46396) obtained from Active motif, Carlsbad, CA (2) for FOXO1.

EMSA. The complimentary oligos (CTAGATGGTAAACAACTGTGACTAGTAGAACACGG) containing the FOXO recognition element (the underlined section, (FRE))(3) were obtained in two sets from Integrated DNA technologies, Coraville, IA. One set was labeled with biotin at both ends (i.e., 3'and 5') and the other set was not labeled. We annealed each set into double stranded DNA and subsequently incubated 20 fmol of biotinylated double stranded DNA with 10 µg of diaphragm nuclear extracts; these reactions were carried out in the following binding buffer—40 mM Tris-HCl, pH 7.5, 5 mM KCl, 2.5 % glycerol, 0.1 mm EDTA, 1.0 mM DTT, 0.05% NP40 and 50 ng/ml of polydeoxyinosinate polydeoxycytidylate (Poly (dI.dC)) for 20 min. As a specificity control we simultaneously carried out the DNA-nuclear extract binding testing for competitive inhibition in the presence of 4 pmol of unlabeled DNA.

The DNA-FOXO complexes were separated from free DNA on a 10 % native TBE gel, then transferred to Biodyne Nylone membrane (catalogue no. 77016, Thermo Scientific, Rockford, IL) and the shift of the complexes from free DNA was detected by LightShift® Chemiluminescent EMSA Kit supplied by PIERCE (catalogue no 20148, Rockford, IL).

ELISA. Briefly (2), we incubated the nuclear extract (10 µg/well) with the DNA sequence immobilized in the 96-well plate for 1 hr. After removal of unbound nuclear extract by washing, we determined the amount of nuclear FOXO1 binding to the immobilized DNA by using anti FOXO1 antibody followed by the specific HRP-conjugated secondary antibody. The substrate reaction to HRP was measured at 450 nm. Additionally, we measured the binding in the presence of an excess of free DNA in solution (i.e., competitive inhibition). Specific activity is presented as the difference between the values obtained without and with free DNA.

UBIQUITIN-PROTEIN CONJUGATES

In order to measure the amount of ubiquitin-protein conjugates in the cytoplasm, equal amounts (15 µg) of the case and the control cytoplasmic fractions were resolved on a reducing SDS-PAGE (4-12%). The proteins were transferred to nitrocellulose membranes and probed with anti-ubiquitin antibody (4). Furthermore we detected the level of SOD 1, which served as loading control

ISOLATION OF 26S PROTEASOMES FROM MYOFIBER LYSATES .

Diaphragm myofiber lysate was prepared in lysis buffer—50 mM HEPES (pH 7.5), 5 mM EDTA, 150 mM NaCl and 1% Triton X-100 detergent in the presence of the Complete Protease

Inhibitor cocktail. Proteasome from the lysate was prepared by using the proteasome isolation kit, human (539176) obtained from Calbiochem, Gibbstown, NJ (5) following the manufacturer's instructions. During isolation, ATP at 2mM was added to the lysate to improve the recovery of intact 26S proteasome fraction. The lysate (0.5-1.0 mg) was added to the affinity bead suspension at a concentration of ~1 mg/ml. The suspension was then incubated at 4^{o}C for 2-4 h with constant mixing to keep the affinity beads well suspended avoiding aeration or vigorous mixing. The samples were then centrifuged for 5 seconds at 4^{o}C (~1000 X g), re-suspended in 1ml of lysis buffer pre-cooled to 4^{o}C and centrifuged again. This procedure was repeated three more times. The bead and 26S proteasome precipitate was then suspended in the enzyme assay buffer provided by the proteasome assay kit AK-740, BIOMOL internationals, Plymouth Meetings, PA (6).

Determination of proteolytic activity of 20S proteasome. To determine *in vitro* proteolytic activity of the 20S component of the 26S proteasome, we measured chymotrypsin like activity (7) in the presence of the enzymatic substrate—S-LLVY-AMC—supplied in the proteasome assay kit AK-740, BIOMOL internationals, Plymouth Meetings, PA (6). The affinity-purified 26S proteasome (15 μg) was incubated with the fluorogenic substrate and the rate of catalytic release of the fluorescent product—7-amino-4 methylcoumarin (AMC)—was measured by the fluorescence emission at 440 nm (λ = 380). As a specificity control, the chymotrypsin like activity of the 20S proteasome was measured in the presence of the proteasome inhibitor, MG132.

GENE EXPRESSION

We used the quantitative real-time reverse transcription polymerase chain reaction (qRT-PCR) to measure the expression level of mRNA transcripts for the ubiquitin ligase genes (MuRF-1 and Atrogin-1) and a house keeping gene (β-Actin). Primer-Probe mixes for 5' nuclease qRT-PCR were procured from Taqman® gene expression assays catalog of Applied Biosystems (ABI), Foster City, CA. Briefly, total RNA was isolated from each diaphragm biopsy using Trizol Reagant, Invitrogen, Carlsbad, CA, and purified by RNeasy micro kit, Qiagen, Valencia, CA. The purity and concentration of total RNA were determined by measurement of absorbance at 260 and 280 nm using a Nanodrop ND-1000 spectrophotometer, NanoDrop Technologies, Wilmington, DE. To satisfy our purity criteria, we discarded all RNA samples that did not have a 260/280 ratio between 1.8 and 2.1. To satisfy our criteria for integrity, we required that all RNA used in our experiments have single peaks for the 18S and 28S bands as determined by the Agilent 2100 Bioanalyzer, Agilent Technologies Inc., Palo Alto, CA.

Subsequently, equal amounts of total RNA from each sample were then reverse transcribed into cDNA using oligo(dT) primers, Invitrogen, Carlsbad, CA. These cDNA samples were amplified in an ABI 7900HT real time PCR system (ABI) using the Taqman® gene expression assays (ABI) noted above. PCR amplification was carried out in 20 µL of a reaction mixture consisting of 2X Taqman® gene expression master mix (ABI) and of assays which contained gene specific primer pair and probe mixes. Amplification parameters consisted of 95˚C 10 min hot start DNA polymerase followed by 40 cycles of 95˚C for 10 sec (denaturing) and 60˚C for 15 sec (annealing/extension). Reporter fluorescence intensity was measured at the

end of each 60˚C cycle which reflected new product formation due to breaks in probe. Gene products were analyzed with Sequence Detection Software (ABI, Version 2.2).

We used the Relative Standard Curve Method for computing the gene expression level in each of our diaphragm samples (8). The standard cDNA was prepared by mixing of samples. We then normalized both genes of interest (i.e., Atrogin-1 and MuRF-1) by dividing each of them by the expression level of ACTB—a housekeeping gene.

STATISTICS

Methodology. We made no assumptions about the distributions of our data. Therefore, data are presented as the median, 25^{th}, and 75^{th} percentiles in addition to the maximum and minimum values. For comparisons between case and control measurements, Mann-Whitney tests were used for continuous data, Friedman's test for repeated measures, and Fisher's exact test for categorical variables. Last, Spearman's Rho was used to characterize the relationship between demographic measurements and outcome variables. All differences and relationships were attributed to chance unless they were significant at the 0.05 level.

Presentation of Data We present statistical descriptions as well as comparisons of groups in our Figures by using box-and-whisker plots; the upper and lower lines of each box represent the 25^{th} and 75^{th} percentiles, the horizontal lines in each box represent the median

value, and the upper and lower horizontal “whiskers” represent the maximum and minimum value of each data set. Group comparisons significant at the 0.05, 0.01, and 0.001 levels are indicated by one (*), two (**), and three (***) asterisks, respectively.

B. RESULTS

Validation of equal protein transfer to membrane. Since using two gels placed on our electroblotter and run under identical conditions for our AKT and FOXO1 measurements is a somewhat unconventional technique, we computed the difference in Ponceau total OD of protein bands per lane that were transferred from one gel having 12 lanes and a second gel having 17 lanes. We noted no statistically significant differences between the median protein level per lane on each of the gels. Indeed, the difference between the two medians was approximately 6.5%.

C. FIGURES AND FIGURE LEGENDS

Figure E1: Diaphragm biopsy specimens available for each of measurements in case and control groups.

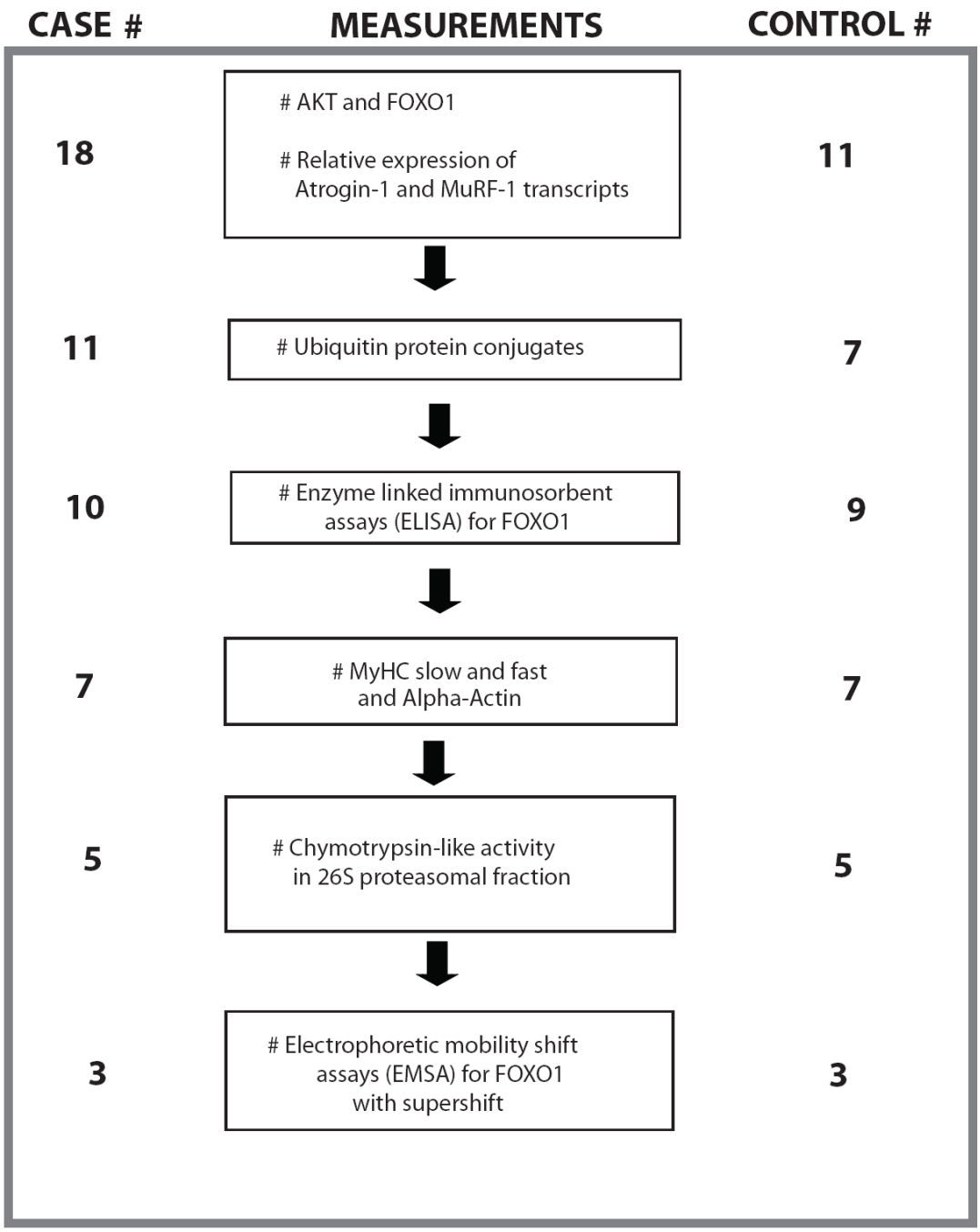
CASE #
MEASUREMENTS
CONTROL #
18
AKT and FOXO1
Relative expression of Atrogin-1 and MuRF-1 transcripts
11
11
Ubiquitin protein conjugates
7
10
Enzyme linked immunosorbent assays (ELISA) for FOXO1
9
7
MyHC slow and fast and Alpha-Actin
7
5
Chymotrypsin-like activity in 26S proteasomal fraction
5
3
Electrophoretic mobility shift assays (EMSA) for FOXO1 with supershift
3

Figure E2: Protein transfer to nitrocellulose membranes and purity of nuclear and cytoplasmic fractions.

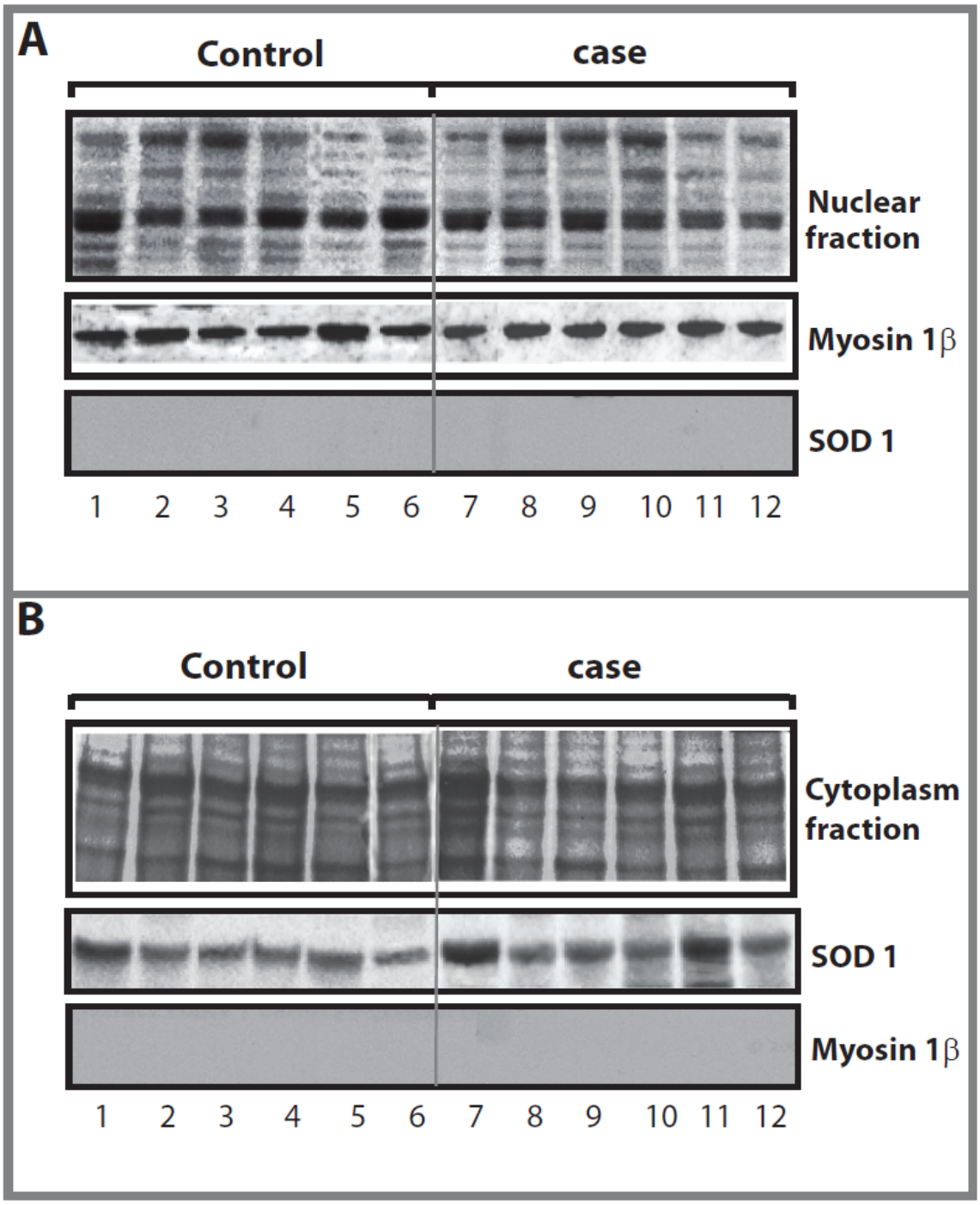

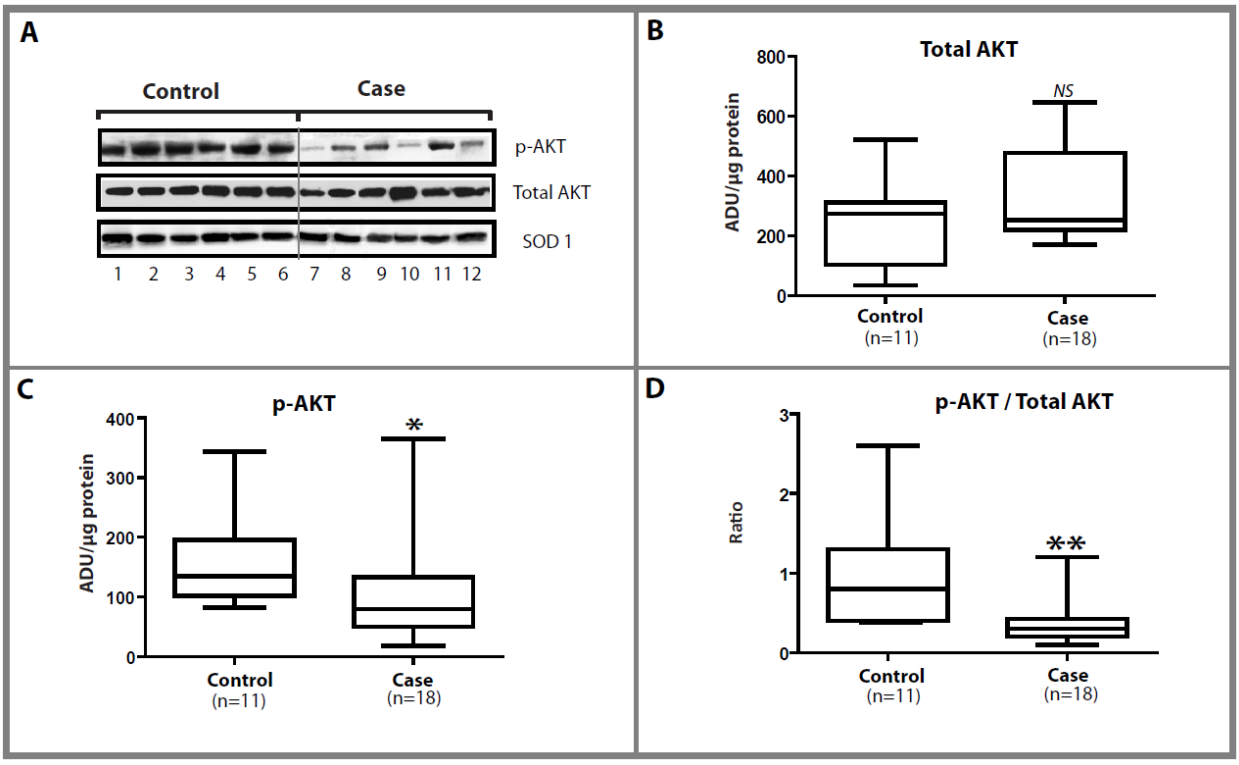

Figure E3: Total AKT and p-AKT in cytoplasmic fractions of case and control diaphragms.

Figure E4: Comparison between case and control Pectoralis major nuclear fractions.

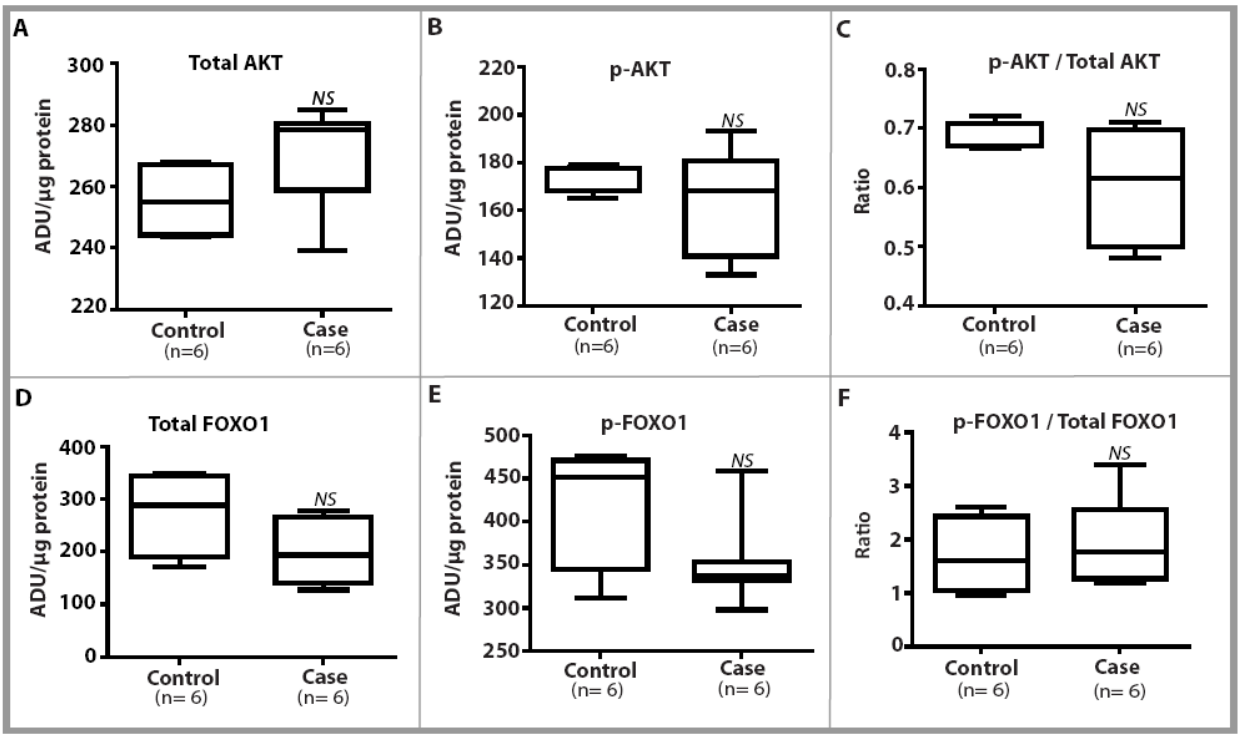

FIGURE LEGENDS (E1-E4)

Figure E1 **Diaphragm biopsy specimens available for each of Measurements in case and control groups.** The rectangles represent the six sequential steps that we used for carrying out our measurements. The Figure shows a progressive depletion of both case and control tissue specimens; therefore, very few samples were available for the later measurements in the study.

Figure E2 **Protein transfer to nitrocellulose membranes and purity of nuclear and cytoplasmic fractions.** Figure E2A displays the results of experiments carried out on nuclear fractions of 6 case and 6 control diaphragms, whereas Figure E2B presents similar data for the cytoplasm fraction of each diaphragm. The upper panel in each Figure represents Ponceau staining of SDS-PAGE gels following transfer to the nitrocellulose membranes. We noted no statistically significant differences between the total amounts of protein (as measured by Ponceau staining) between case and control specimens. Likewise, the middle panels of each figure indicate that case and control specimens did not differ with respect to amounts of the loading controls—amount of myosin 1β for nuclear

fractions and amount of superoxide dismutase 1 (SOD1)for cytoplasm fractions.

The lowest panel in Figure E2A shows the results of staining the nuclear fraction on the membranes for SOD1—the cytoplasm protein. The absence of any SOD1 staining in the lowest panel in this Figure strongly suggests that the nuclear protein fraction is "pure"—i.e., free of contamination by cytoplasm proteins.

The lowest panel in Figure E2B depicts the results of staining the cytoplasm fraction on the membranes for Myosin 1β—the nuclear protein. The absence of any myosin 1β staining in the lowest panel in Figure E2B strongly suggests that the cytoplasm protein fraction is "pure"—i.e., free of contamination by nuclear proteins.

Figure E3: **Total AKT and p-AKT in cytoplasmic fractions of case and control diaphragms.** Figure E3A shows representative case (n=6) and control (n=6) immunoblots. In comparison to controls, the immunoblots demonstrate that cases exhibited a decrease in p-AKT (P=0.002), a decrease in p-AKT/Total AKT ratios (P=0.004) and no statistically significant differences with respect to Total AKT. The SOD 1 measurements in the lowest panel of Figure 3A served as our loading control; the SOD measurements show equal protein loads in all lanes.

We carried out these 3 measurements on a total of 18 cases and 11 control subjects and these group comparisons are shown in Figures E3B, E3C, and E3D. As shown by the statistical symbols, the results were very similar to the representative sample data shown in Figure 4A in the main manuscript. **Definition of statistical symbols:** Group comparisons significant at the 0.05, 0.01, and 0.001 levels are indicated by one (*), two (**), and three (***) asterisks, respectively.

Figure E4: **Comparison between case and control Pectoralis major nuclear fractions of biopsies with respect to p-AKT, Total AKT, p-AKT/Total AKT, pFOXO1, Total FOXO1and p-FOXO1/Total FOXO1.** Figures E4A to E4F indicate that no statistically significant differences were noted between case (n=6) and control (n=6) biopsies. We used Myosin 1β as loading control. See the lower panels of Figure 7A and 7B in the main manuscript; they show equal protein loads in all lanes. **Definition of abbreviation:** NS=not statistically significant at p= 0.05.

D. TABLES

Table E1: Summary of Demographic Characteristics, Cause of Brain Death or Reason for Surgery, and Medical History of Case and Control Subjects*.

Case subjects	Age (yr)	Gender	BMI	Reason for Cause of Brain Death or Surgery	Medical History
1	56	F	26	Stroke	Smoked 80 pack/yr
2	49	M	24	Motor vehicle accident	Hypertension, peptic ulcer disease, depression, hypogonadism, smoker
3	40	M	29	Stroke	Hypothyroid, arteriovenous malformation in brain-- treated 2 years ago
4	45	M	32	Stroke	Hypertension, ethyl alcohol abuse, drug abuse
5	17	F	24	Motor vehicle accident	None
6	26	M	28	Cardiorespiratory arrest	Seizure disorder
7	53	F	45	Stroke	Hypertension, type 2 diabetes mellitus, gastroesophageal reflux disease, atrial fibrillation (new onset)
8	19	M	24	Cardiorespiratory arrest	Seizure disorder with implanted pacemaker
9	75	M	33	Stroke	Hypertension, type 2 diabetes mellitus
10	54	M	36	Cardiorespiratory arrest	Hypertension, Gout, extensive alcohol and

Case subjects	Age (yr)	Gender	BMI	Reason for Cause of Brain Death or Surgery	Medical History (Continued)
					tobacco abuse
11	33	F	44	Suicide (Drug overdose-opiates, ETOH, barbiturate)	Drug and ethyl alcohol abuse, metronidazole and ceftriaxone for vaginitis
12	21	M	26	Head Trauma	Non-smoker
13	46	F	27	Cardiorespiratory arrest associated with status asthmaticus	Asthma, HTN, Non smoker
14	37	M	21	Suicide (hanging)	Cocaine abuse, 8 pk/year smoker (quit 6 yrs ago)
15	55	M	31	Stroke	Type 2 diabetes mellitus, hypertension, 33 pk/yr smoker (quit 10 yrs ago)
16	43	F	28	Cardiorespiratory arrest	Alcohol and cocaine) abuse, Active smoker (>10 pk/yr)
17	35	M	27	Gunshot wound to head	Depression, active smoker (3.5 pk/yr)
18	58	F	36	Stroke	Hypertension, COPD, hypothyroidism, schizoaffective disorder, bipolar disorder, active smoker (25 pk/yr), obesity, history of steroid therapy

Control Subjects	Age (yr)	Gender	BMI	Reason for Cause of Brain Death or Surgery	Medical History (Continued)
1	45	F	24	Stage 1 non-small cell cancer of lung	History of melanoma
2	76	M	27	Stage I non-small cell cancer of lung	Coronary artery disease with history of myocardial infarction and coronary artery bypass surgery, prostate carcinoma treated with radiation therapy, pipe smoker (quit 30 yr ago)
3	58	F	27	Stage 1 non-small cell lung cancer	History of breast cancer
4	54	F	23	Ganglioneuroma	Glaucoma, seasonal allergies, nonsmoker
5	25	F	27	Ganglioneuroma	Gallstones, non-smoker
6	41	F	26	Hamartoma	Herniated lumbar disks, dysfunctional uterine bleeding , smoked 24 pack/yr (quit 2yr ago)
7	21	F	18	Bronchogenic cyst (benign)	Bipolar Disorder, Active smoker 9 packs/year
8	20	F	20	Pulmonary sequestration	Recurrent severe respiratory infection in the right lower lobe, Non-smoker
9	64	M	34	Pulmonary nodules (Benign)	Cholecystitis with septic shock 3 months

Control subjects	Age (yr)	Gender	BMI	Reason for Cause of Brain Death or Surgery	Medical History (Continued)
					ago, type II Diabetes, hypertension, 45 pk/yr history of smoking (quit 3yrs ago)
10	44	F	20	Right middle lobe syndrome	Recurrent right middle lobe infections. Had bronchiectasis of right middle lobe. Non-smoker
11	41	F	21	Pulmonary nodules (benign)	Active smoker 10 pk/yr.

*All control subjects had either normal values for spirometry or values consistent with mild to moderate obstructive lung disease. BMI denotes body mass index (defined as the weight in kilograms divided by the square of the height in meters).

Table E2: Summary of Ventilator Settings, Arterial Blood Gas Measurements, and Vital Signs for Control and Case Subjects.¤

Measurement	**Control Subjects (N=11)**	**Case subjects (N=18)**	**P Value**
Ventilator settings and related measurements			
Time of Mechanical ventilation (hours)	2.5(2.0,3.0)	26(22,45)	<0.001
Tidal Volume(ml/kg of body weight)	------	600(550,763)	------
Ventilation frequency (Breaths/min)	15(10,16)	14(12,16)	0.753
PEEP (cm H_2O)	0(0,0)	5(5,5)	<0.001
FiO_2 (%)	91(88,100)	50(40,60)	<0.001
SaO_2 (%)	100.0(99.5,100.0)	98.0(93.7,99.7)	0.018
$P_{ET}CO2$ (mm Hg)	32(30,37)	------	------
$PaCO_2$ (mm Hg)	------	32.3(31.4,44.3)	------
Arterial pH (units)	------	7.39(7.34,7.45)	------
PaO_2/FiO_2†	------	345(242,459)	------

Measurement	Control Subjects (N=11)	Case subjects (N=18)	P Value (Continued)
Vital signs			
Systolic pressure (mm Hg)	105(95,125)	133(124,150)	0.015
Diastolic pressure (mm Hg)	60(58,73)	79(70,80)	0.021
Heart rate (beats/min)	80(64,81)	95(89,107)	0.005
Body temperature (C°)	35.6(35.5,36.1)	37.0(36.3,37.4)	0.045

¤ The values are presented as the median, and 25^{th}, 75^{th} percentiles in parenthesis. FiO_2 denotes fractional concentration of inspired oxygen, $PaCO_2$ arterial carbon dioxide pressure, PEEP positive end-expiratory pressure, $P_{ET}CO_2$ end-tidal carbon dioxide pressure, and SaO_2 arterial oxygen saturation. All control subjects had either normal values for spirometry or values consistent with mild to moderate obstructive disease.

† These measurements were made at an FiO_2 of 1.0.

E. REFERENCES:

1. Levine S, Nguyen T, Taylor N, Friscia ME, Budak MT, Rothenberg P, Zhu J, Sachdeva R, Sonnad S, Kaiser LR, et al. Rapid disuse atrophy of diaphragm fibers in mechanically ventilated humans. *N Engl J Med* 2008;358:1327-1335.

2. McClung JM, Kavazis AN, Whidden MA, DeRuisseau KC, Falk DJ, Criswell DS, Powers SK. Antioxidant administration attenuates mechanical ventilation-induced rat diaphragm muscle atrophy independent of protein kinase b (pkb akt) signalling. *J Physiol* 2007;585:203-215.

3. Zhang X, Gan L, Pan H, Guo S, He X, Olson ST, Mesecar A, Adam S, Unterman TG. Phosphorylation of serine 256 suppresses transactivation by fkhr (foxo1) by multiple mechanisms. Direct and indirect effects on nuclear/cytoplasmic shuttling and DNA binding. *J Biol Chem* 2002;277:45276-45284.

4. Mimnaugh EG, Bonvini P, Neckers L. The measurement of ubiquitin and ubiquitinated proteins. *Electrophoresis* 1999;20:418-428.

5. Kopp F, Hendil KB, Dahlmann B, Kristensen P, Sobek A, Uerkvitz W. Subunit arrangement in the human 20s proteasome. *Proc Natl Acad Sci U S A* 1997;94:2939-2944.

6. Stein RL, Melandri F, Dick L. Kinetic characterization of the chymotryptic activity of the 20s proteasome. *Biochemistry* 1996;35:3899-3908.

7. Shanely RA, Zergeroglu MA, Lennon SL, Sugiura T, Yimlamai T, Enns D, Belcastro A, Powers SK. Mechanical ventilation-induced diaphragmatic atrophy is associated with oxidative injury and increased proteolytic activity. *Am J Respir Crit Care Med* 2002;166:1369-1374.

8. Larionov A, Krause A, Miller W. A standard curve based method for relative real time pcr data processing. *BMC Bioinformatics* 2005;6:62.